Thresholds in transient dynamics of signal transduction pathways

Katja Rateitschak, Olaf Wolkenhauer

www.elsevier.com/locate/yjtbi

Thresholds in transient dynamics of signal transduction pathways

Katja Rateitschak, Olaf Wolkenhauer

PII: S0022-5193(10)00060-3
DOI: doi:10.1016/j.jtbi.2010.02.001
Reference: YJTBI 5854

To appear in: *Journal of Theoretical Biology*

Received date: 1 October 2009
Revised date: 1 February 2010
Accepted date: 2 February 2010

Cite this article as: Katja Rateitschak and Olaf Wolkenhauer, Thresholds in transient dynamics of signal transduction pathways, *Journal of Theoretical Biology*, doi:10.1016/j.jtbi.2010.02.001

Thresholds in transient dynamics of signal transduction pathways

Katja Rateitschak*, Olaf Wolkenhauer

Systems Biology and Bioinformatics Group
University of Rostock
18051 Rostock, Germany
katja.rateitschak@uni-rostock.de
olaf.wolkenhauer@uni-rostock.de

www.sbi.uni-rostock.de

February 1, 2010

Abstract

Transient dynamics of signal transduction pathways play an important role in many biological processes, including cell differentiation, apoptosis, metabolism and DNA damage response. Recent examples of quantitative methods to characterize transient signals include transient metabolic control coefficients and finite time Lyapunov exponents. In our work we compare these quantitative methods to characterize transient phenomena and specifically discuss their predictive power for three examples. We focus on the identification of thresholds that separate different transient dynamic behaviors. Our investigation leads to the following results: The spectrum of the finite-time Lyapunov exponents unambiguously and reliably identifies putative thresholds in transient dynamics. Metabolic control coefficients do not reliably detect all thresholds and suffer from false positives.

Key words: signal transduction, transient dynamics, Lyapunov exponents, metabolic control coefficient, Hill equation, relative instability exponent

*Corresponding author. Tel: +49 381 498 7682, Fax: +49 381 498 7572

1 Introduction

The behavior of cellular processes can be classified into steady state and transient dynamics, whereby we include biochemical oscillations with constant amplitude as examples of steady state processes. While steady state processes are most important in metabolic systems [1], transient dynamics play an important role in cell communication [2, 3, 4, 5, 6, 7].

Transient dynamics describe the transition from some initial state of the system into a steady state. For an understanding of signaling pathways and their targets transient dynamics are often more important than steady state dynamics as demonstrated by the following examples: Aldridge et al. [2] have established a mathematical model which describes the regulation of active caspase 3 dynamics in apoptosis. The temporal duration depends on the initial condition (concentration) of the protein xiap. Bolouri and Davidson [3] have shown by mathematical modelling that genes are activated successively in a regulatory network cascade, long before steady states are attained. The EGFR stimulated MAPK cascade in the PC12 cell line shows a transient activation of ERK with a peak at 5 min and a return to its basal level after 30 min, which leads to cellular proliferation [4]. Using mathematical modelling Cheong et al. [5] have predicted that the dynamic profile of the IKK signal must transiently peak at all TNFα doses in order to generate the observed NFκB activity which they could experimentally validate.

Aldridge et al. have employed direct finite-time Lyapunov exponents to identify domains in the transient dynamics of high sensitivity to initial conditions [2]. These separatrices delineate regions with different transient dynamics and can be considered as a threshold. Furthermore, for the activation of a signalling pathway often threshold concentrations of proteins are required to prevent the unintentional activation of signalling pathways through random fluctuations.

The relevance of thresholds in biology is demonstrated by a large number of publications about ultrasensitive responses ranging from Goldbeter [8] and Ferrell [9] to the recent work of Buchler [10]. Ferrell has concluded, on the basis of experimental data, that the MAPK cascade is optimized to convert a graded input into a switch-like output [9]. Ultrasensitive responses leading to sigmoidal stimulus-response curves have been related to activation thresholds of biochemical networks in the literature [8, 11, 12, 13, 14, 15, 16, 17]. Experimental measurements in networks with multiple phosphorylations have shown that the stimulus has to exceed a threshold concentration to activate downstream events [10, 11, 12, 13]. Mathematical models for the MAPK cascade with dual phosphorylation [14] and general models for multisite phosphorylations [17] have shown that multisite phosphorylation give rise to more threshold like responses that single site phosphorylation. So far, however, mathematical modelling has focused on network properties leading to sigmoidal stimulus-response curves in the steady state dynamics.

In small networks, stimulus-response curves of the transient and steady dynamics can be studied in detail, leading to the identification of putative thresholds. In larger biochemical networks the identification of putative thresholds would become very time consuming because the network components could show sigmoidal-stimulus response curves during different time intervals. Therefore quantitative measures to identify putative thresholds in transient dynamics are required. They should be designed such that an inspection of trajectories is not necessary, i. e. they should deliver initial conditions (concentrations) of proteins and respective time intervals where a response shows a threshold. Recent examples of quantitative methods to characterize transient signals include transient metabolic control coefficients (MCC) [18, 19] and finite time Lyapunov exponents (FTL) [2]. We here focus on system structures that generate thresholds in transient dynamics and investigate quantitative measures to identify such thresholds.

The outline of this paper is as follows. Following an introduction to MCCs and FTLs, we define thresholds in cellular signaling, discuss their properties and argue for the need of quantitative measures to identify them in transient dynamics. We then study two model structures that can generate thresholds in their transient response and we compare quantitative measures to identify thresholds in the transient dynamics. We first extend the analysis of thresholds by FTLs in an apoptosis decision network [2] by calculating the three largest FTLs and the MCCs. Next, we study a gene transcription network as an alternative model structure to generate thresholds in transient dynamics. Our analysis of the gene transcription network has motivated us to analytically quantify the threshold of a Hill equation and to discuss an alternative measure which combines properties of the FTLs and the MCCs.

Finally the results of our comparative study will lead us to an evaluation of the investigated quantitative measures regarding their ability to identify thresholds in transient signaling.

2 Quantitative measures to characterize transient dynamics

Metabolic control coefficients (MCC) measure the relative response of a state variable x_i, with respect to the relative perturbation by state variable x_j. They are a standard quantitative measure in sensitivity analysis [1]. MCCs can also be calculated for finite times as described in [18, 19]. They are defined by

$$C\big(x_i(t), x_j(0)\big) = \frac{\partial \log x_i(t)}{\partial \log x_j(0)} \ . \tag{1}$$

Comparing the influence of a perturbation at $t = 0$ on different state variables

at $t > 0$ it is useful to consider relative changes of state variables because the values of different state variables can have different orders of magnitude. Thus control coefficients for different pairs (i, j) can be compared. In general one uses the same percentaged perturbation for all $x_j(0)$ resulting in the same denominator for all $C\big(x_i(t), x_j(0)\big)$. To perturb simultaneously initial conditions of several state variables, global approaches have to be applied [20], which is not the focus of this work.

The MCC in Eq. (1) is also called "concentration control coefficient". Replacing in the denominator the initial condition $x_j(0)$ by a parameter, for example a reaction constant, leads to another type of concentration control coefficient. The concentration control coefficients can be calculated for the transient dynamics as well as in the steady state. In addition, flux control coefficients have been introduced to quantify the control of the flux of a metabolic system in the steady state [1].

Lyapunov exponents measure the exponential divergence between a reference trajectory and d orthogonal perturbations to the trajectory, where d is the dimension of the related mathematical model which is equal to the number of state variables [21]. Finite time Lyapunov exponents (FTL) have been introduced to quantify dynamical instabilities over a finite interval of time [22, 23, 24, 25]. They depend on time and on the initial conditions of the dynamical system. The FTLs $\lambda_i(t, x(0))$, $i = 1, \ldots, d$ can be calculated from the numerical solution of the ordinary differential equations (ODE) for a finite time t and initial state $x(0)$ at $t = 0$:

$$\begin{aligned} \dot{x} = f(x) \quad \dot{u} = \frac{df}{dx} u \\ \lambda_i\big(t, x(0)\big) = \frac{1}{2t} \log\left(\Lambda_i(u^T \cdot u)\right) \end{aligned} \tag{2}$$

where $\dot{x}$ denotes a system of ODEs, and $\dot{u}$ a matrix differential equation for d initially orthonormal perturbation vectors which are the columns of the matrix u, and u^T being the transpose of u and $\Lambda_i(u^T \cdot u)$ denoting the eigenvalues of $u^T \cdot u$. Alternatively, λ_i can be calculated directly from differences between trajectories and initially perturbed trajectories [2].

The number of Lyapunov exponents is equal to d and the whole set of them is also called the Lyapunov spectrum. The largest Lyapunov exponent quantifies the exponential divergence of the most unstable direction and the lower Lyapunov exponents quantify the exponential divergence in the $d - 1$ orthogonal directions.

Comparing the definitions of MCC and FTL the differences can be summarized as follows: The FTLs identify the most unstable direction of the state space and the stability in all orthogonal directions on the basis of absolute distances between the trajectory and perturbed trajectories. The MCCs measure the response-

perturbation ratio on the basis of relative changes of state variables.

Recent experimental results show that biological responses can be absolute or relative: In EGF stimulated H1299 cells the absolute change of ERK2 response varies in different cells but the relative response is the same in different cells [26]. An absolute response mechanism seems to occur in some bacterial systems [27].

In our study we have numerically calculated the MCC according to Eq. (1) and the FTL according to Eq. (2). We have coded the calculations in Matlab [28]. For the eigenvalues in Eq. (2) we have also coded an RQ decomposition but our results do not depend on it. The Matlab code can be obtained from the authors upon request.

3 Thresholds in transient dynamics

Cells respond to changes in protein concentrations, which suggests that concentration changes should be the basis for a definition of thresholds in cellular signaling. As it has been discussed in the introduction sigmoidal stimulus-response curves have been related to activation thresholds of biochemical networks [8, 11, 12, 13, 14, 15, 16, 17]. So far, experimental and modeling efforts have focused on sigmoidal stimulus-response curves in the steady state.

We suggest that a threshold value of a sigmoidal stimulus response curve can be defined by the stimulus that corresponds to the inflection point of the response curve. An alternative definition could be based on the highest curvature of the stimulus-response curve. Due to the fact that an interval of initial conditions can have the same curvature, we can only determine a threshold interval instead of a threshold value. The two suggested definitions of a threshold contain only information about the level of a stimulus at which a threshold exists but they do not contain information about its shape. The threshold encoded by the shape of a sigmoidal stimulus-response curve can vary from very steep thresholds, approaching a switch, to smoother thresholds with a lower steepness.

A typical sigmoidal stimulus-response curve, found in many references, is shown in the first column of Fig. 1. In the second column a sigmoidal stimulus-response curve is shown, where the response increases without saturation. Another possibility is a hyperbolic stimulus-response curve, where the response increases little below the interval of the highest curvature, while above, it increases without saturation. We call this interval of the highest curvature a "hyperbolic threshold", illustrated in the third column of Fig. 1. These definitions can be applied to steady states as well as to transient dynamics.

We here consider a stimulus as either some external input, say extracellular ligands, as well as initial condition (concentrations) of intracellular signaling proteins [15]. An example for an extracellular stimulus is the gene transcription network

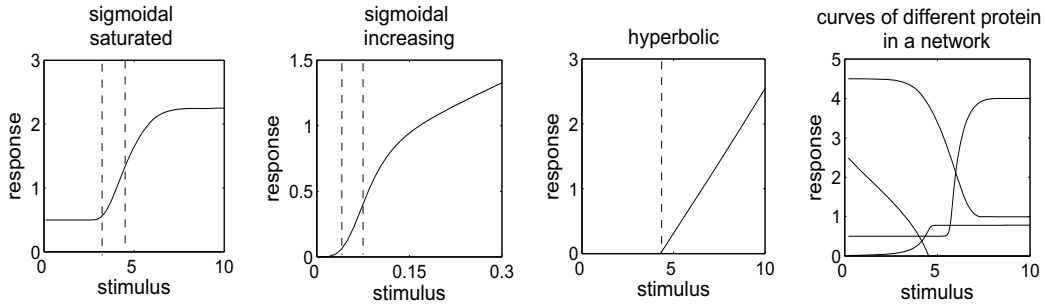

Figure 1: Thresholds in stimulus-response curves. The possible thresholds are indicated by dashed lines. For the two sigmoidal curves the threshold can be defined by the inflection point or by the interval with the highest curvature. For the hyperbolic curve the threshold can be defined by the interval with the highest curvature. The right-most column shows a situation in a biochemical network with stimulus-response curves of different proteins.

studied in this work. The transient intracellular response can also sigmoidally depend on the initial condition (concentration) of an intracellular signaling protein as in the apoptosis decision network investigated further below. Both types of "stimuli" as thresholds have been investigated in [15]. If there is no specific interest in certain network components, one should vary the initial conditions of all variables to identify thresholds. In our two studied examples we have restricted ourselves to one or two initial conditions because our objective was to compare FTL and MCC and not a detailed analysis of the models.

In transient signaling, threshold values can depend on time, which has to be considered in the discussion about the biological relevance for a predicted threshold. The amplitude of a stimulus-response curve is also essential for this evaluation. If the amplitude is too small, then the threshold effect can be lost by noise. As raised in the introduction, in larger biochemical networks the identification of putative thresholds would become very time consuming because the network components could show sigmoidal-stimulus response curves during different time intervals. The activation of a signaling pathway at the membrane-bound receptor requires a particular threshold concentration of the stimulus. For downstream components their threshold value may be higher than further up in the network or a threshold values has to be passed to switch off an inhibitor of the pathway, as shown in the right-most column of Fig. 1 (see the related discussion in [29]). Therefore quantitative measures to identify putative thresholds in transient dynamics and concepts to predict their downstream consequences are required.

Quantitative measures with an extreme value at the inflection point, or during the interval with the highest curvature, would allow a fast identification of putative

thresholds in larger biochemical networks. These predictions would then have to be confirmed in experiments. In the case of different threshold values the analysis of the related downstream networks will answer the question whether the threshold to activate a downstream event is an integrated response.

Summarizing our discussion, we seek quantitative measures that identify the inflection point or the interval of the highest curvature of a stimulus-response curve. To evaluate whether FTLs or MCCs are appropriate we have chosen three examples, which are simple enough to study in detail the dynamics of the trajectories and stimulus-response curves but which at the same time are complex enough to show thresholds in their transient dynamics. In our work we focus on the identification of thresholds, while in other works quantitative measures to analyze the steepness of sigmoidal stimulus-response curves have been investigated [16, 29].

4 Apoptosis decision network

A mathematical model describing the kinetics of an apoptosis decision network has been presented in [2]. The respective reaction network is shown in Fig. 2 and the variables are summarized in Table 1.

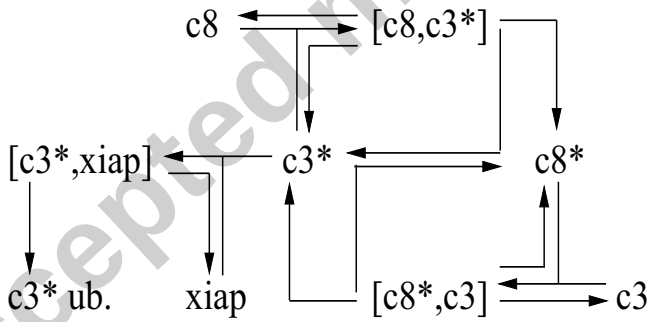

Figure 2: Apoptosis decision network. Figure adopted from [2].

The mathematical model includes interactions of the proteins caspase3, caspase8 and xiap: It describes the activation of $c8$ by $c3^*$ (the asterisk denotes the active form) and the activation of $c3$ by $c8^*$. The model represents a mutual activation cycle. In addition, the model includes the *xiap*-dependent degradation of $c3^*$.

The model does not include an external stimulus inducing the transient response. Aldridge et al. [2] have investigated the transient dynamics in dependence on the initial conditions of network components to identify critical initial concentrations for the survival/death decision. In addition they have shown that a steady

Name	Shorthand
caspase8	$c8$
caspase8*	$c8^*$
caspase3	$c3$
caspase3*	$c3^*$
complex of caspase8* and caspase3	$[c8^*, c3]$
complex of caspase8 and caspase3*	$[c8, c3^*]$
xiap	$xiap$
complex of xiap and caspase3*	$[c3^*, xiap]$

Table 1: Assignment of names for variables.

state analysis does not reveal the critical initial concentrations for a survival/death decision. The authors have identified a threshold for the survival/death decision by a maximum of the largest FTL for a critical value of $xiap(0)$. They reported that the final decision between cell survival and controlled cell death critically depends on the temporal duration of the activity of $c3^*$ in living cells. A short duration leads to survival, while a long duration leads to cell death.

We here extend the analysis of this mathematical model by calculating the three largest Lyapunov exponents and the MCCs and by comparing these quantities with the dynamics of this network. We begin with a reduction of the original eight ODEs, Eqs. (1-8) of [2] to six ODEs, by applying conservation equations for $c8$ and $xiap$. This leads to the following set of equations:

$$\begin{aligned}
\frac{d}{dt}c8^* &= k_{d2}\cdot[c8,c3^*] + (k_{d3}+k_{d4})[c8^*,c3] - k_3\cdot c3\cdot c8^* \\
\frac{d}{dt}c3 &= k_{d3}\cdot[c8^*,c3] - k_3\cdot c3\cdot c8^* \\
\frac{d}{dt}c3^* &= k_{d4}\cdot[c8^*,c3] + (k_{d1}+k_{d2})\cdot[c8,c3^*] + k_{d5}\cdot[c3^*,xiap] \\
&\quad - k_1\cdot c3^*\cdot c8 - k_5\cdot c3^*\cdot xiap \\
\frac{d}{dt}[c8,c3^*] &= k_1\cdot c3^*\cdot c8 - (k_{d1}+k_{d2})\cdot[c8,c3^*] \\
\frac{d}{dt}[c8^*,c3] &= k_3\cdot c3\cdot c8^* - (k_{d3}+k_{d4})\cdot[c8^*,c3] \\
\frac{d}{dt}xiap &= (k_{d5}+k_{d6})[c3^*,xiap] - k_5\cdot c3^*\cdot xiap
\end{aligned} \tag{3}$$

	Value	Units	Variable	Initial value	Units
k_1	$2.67{\cdot}10^{-9}$	$cell \cdot (s \cdot molecules)^{-1}$	$c8$	$3.5 \cdot 10^5$	$molecules/cell$
k_{d1}	0.01	s^{-1}	$c8^*$	$5 \cdot 10^4$ or 10^5	$molecules/cell$
k_{d2}	0.008	s^{-1}	$c3$	$2.6{\cdot}10^5$	$molecules/cell$
k_3	$6.8{\cdot}10^{-8}$	$cell \cdot (s \cdot molecules)^{-1}$	$c3^*$	100	$molecules/cell$
k_{d3}	0.05	s^{-1}	$[c8^*, c3]$	100	$molecules/cell$
k_{d4}	0.001	s^{-1}	$[c8^*, c3]$	100	$molecules/cell$
k_5	0.00007	$cell \cdot (s \cdot molecules)^{-1}$	$xiap$	10^3 to 10^5	$molecules/cell$
k_{d5}	0.0000167	s^{-1}	$[c3^*, xiap]$	100	$molecules/cell$
k_{d6}	0.000167	s^{-1}			

Table 2: Apoptosis model: Parameter values and initial conditions.

where the conservation equations are given by

$$\begin{aligned} \overline{c_8} &= c8 + c8^* + [c8, c3^*] + [c8^*, c3] \\ \overline{xiap} &= xiap + [c3^*, xiap] \ . \end{aligned} \tag{4}$$

The parameters and the initial values of the variables, including respective units are the same as in [2] (See Table 2).

We study the dynamics of the network components for different initial conditions of $xiap$, the inhibitor of $c3^*$, and thus a critical regulator of the survival/death decision [2]. The trajectories of all network components for eleven different $xiap(0)$ are shown in Fig. 3. They show a more or less pronounced clustering into two groups for each network component, thus indicating thresholds. Groups with fully overlapping trajectories are annotated by "$*$". On the basis of the trajectories we have chosen time points between $t = 6h$ and $t = 18h$ to study transient dynamics of the system.

In Fig. 4 we compare the concentrations of the network components (first row) with the FTLs λ_i (second row) and with the MCCs $C(x_i, x_j)$ (third row) as a function of $xiap(0)$ (abscissa) for the three chosen time points (columns) during the transient signal. We call the curves in the first row of Fig. 4 stimulus-response curves, to use standard notation though the "stimulus" is the initial condition $xiap(0)$ in our study. The proteins $c8^*$ and $c3$ show a sigmoidal stimulus-response curve in agreement with the clusters of the related trajectories in Fig. 3 and thus each curve has an individual sigmoidal threshold. The intervals of the stimulus, which corresponds to the increasing part of the stimulus-response curve, are partially overlapping within a small $xiap(0)$ interval whose position is independent of

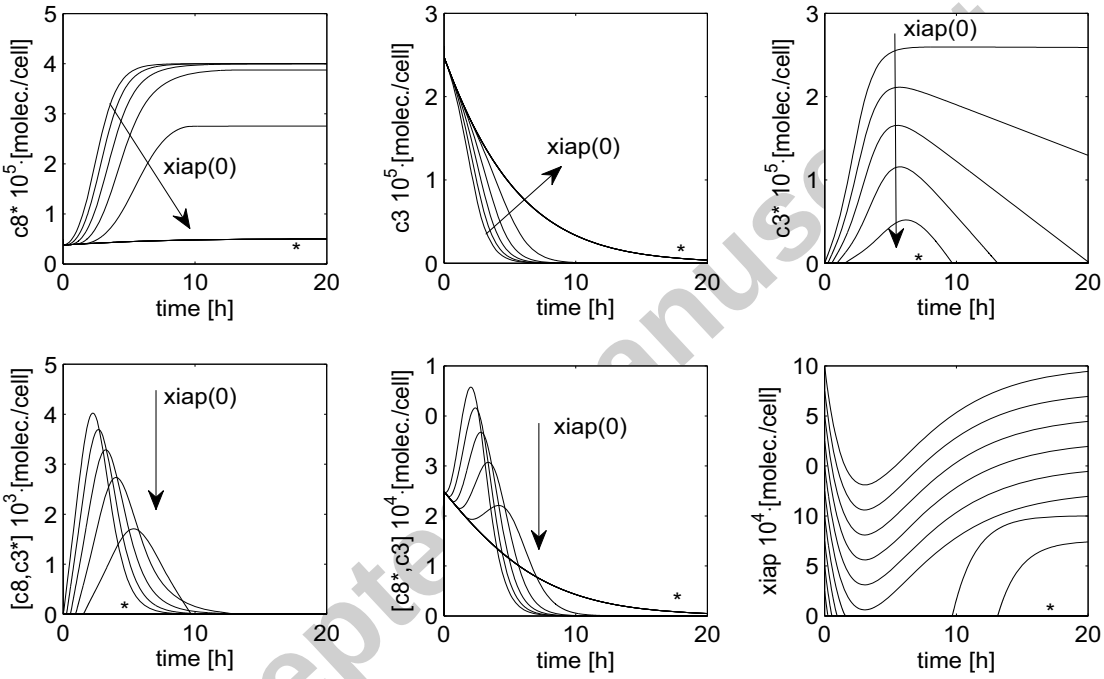

Figure 3: Apoptosis decision network. Trajectories of the network components for $xiap(0) = 0$ $molecules/cell$, 10^4 $molecules/cell$, $2 \cdot 10^4$ $molecules/cell \ldots, 10^5$ $molecules/cell$. An arrow indicates the direction of increasing $xiap(0)$. A "*" indicates a cluster of overlapping trajectories.

time[1]. Thus their inflection points and the intervals with the highest curvature, where the response raises, are in close vicinity. The three components are directly linked in the network of Fig. 2.

The curve of *xiap* is sigmoidal too and for $t = 6h$ also the curve of $c3^*$. For $t = 12h$ and $t = 18h$, $c3^*$ has not a sigmoidal but a hyperbolic threshold. The sigmoidal threshold of *xiap* and the hyperbolic threshold of $c3^*$ are in close vicinity[2]. Their positions depend on time and are located around different $xiap(0)$, compared to the sigmoidal threshold of $c8^*$ and $c3$ for $t = 12h$ and $t = 18h$.

Our results for the FTLs are shown in the second row of Fig. 4, where only the three largest FTLs are shown[3]. The maximum of the largest FTL λ_1 is located at a $xiap(0)$, which is close to the inflection points of the overlapping stimulus-response curves for $c8^*$ and $c3$. The stimulus-response curve of $c8^*$ has the largest amplitude, while the steepness of the three curves are similar. Thus $c8^*$ contributes most to the maximum of λ_1, although the largest FTL has identified a sigmoidal threshold as an integrated response of $c8^*$, $c3$, and $[c3, c8^*]$. The profile of λ_1 for $t = 6h$ agrees with the result in Fig. 4 of [2].

The second largest FTL has a maximum at a different critical $xiap(0)$, which is found close to the thresholds for $c3^*$ and *xiap*. The dynamics of the protein $c3^*$ contribute probably only at $t = 6h$ to the maximum of the second largest FTL because for the other two time points its stimulus-response curve is hyperbolic. The value of this critical $xiap(0)$ decreases with time, in contrast to the case above. This means, the longer the damage persists, the higher becomes the chance for survival. This sounds unrealistic and thus it is questionable whether the $xiap(0)$, leading to a maximum of the second largest Lyapunov exponent, is a true biological threshold. On the other hand, for the opposite case, it could be realistic that the chance for survival decreases with time.

The second largest FTL is negative and thus the respective direction in state space is stable. A maximum of a negative FTL indicates minimal stability. Related stimulus-response curves are sigmoidal and initial conditions with the point of inflection form a threshold according to our definition. These relations cannot be directly inferred from Fig. 4 due to several interacting proteins. In Appendix B we present a one-dimensional example which allows the reader to follow this fact.

Our results for the MCCs leading to the largest maxima and minima at critical $xiap(0)$ are shown in the third row of Fig. 4. We have independently perturbed

[1]The sigmoidal curve of $[c8^*, c3]$ has its inflection point within this interval too but it has a too small response amplitude and is thus not visible in Figure 4.

[2]The curve of $[c8, c3^*]$ has a maximum at the same $xiap(0)$ but it is too small and is thus not visible in this figure.

[3]The three smallest FTLs could not be determined due to numerical problems with orthonormalization of the respective tangent vectors. We have used the RQ decomposition for orthonormalization.

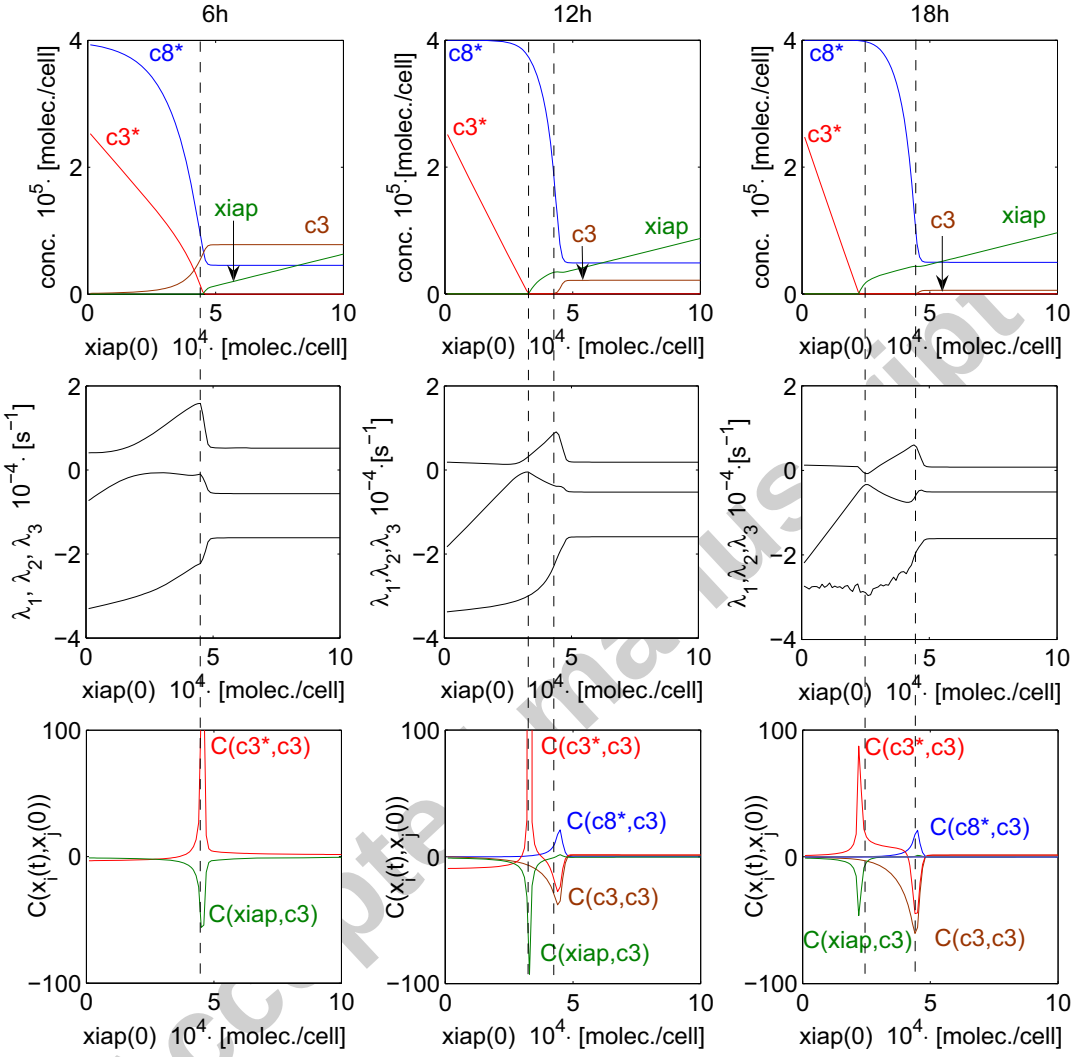

Figure 4: Apoptosis decision network. Quantitative measures to characterize transient dynamics. $c8^*(0) = 5 \cdot 10^4$ *molecules/cell*, abscissa: $xiap(0)$. First row: stimulus-response curves. Second row: FTLs and third row: Profiles of MCCs which lead to largest maxima and minima at the two critical $xiap(0)$ are shown. Columns: different time points. Dashed lines have been added for a better comparison of the maxima of FTLs, extreme values of MCCs and thresholds in stimulus-response curves. Same colors are chosen for the same response variable in the first and third row. The quantified threshold values are summarized in Table 3 in Appendix A.

the initial values of all cellular components by one percent and then calculated the resulting responses for each $xiap(0)$. Comparing the results for the MCCs with the results for the FTLs and the results for the stimulus-response curves, shows that the MCCs have extreme values for the two values of $xiap(0)$ at which the first and second largest FTL have their maximum. Perturbations in $c3(0)$ cause most sensitive responses. The global maximum is the MCC, $C(c3^*, c3)$, found at the critical $xiap(0)$ with the maximum of the second largest Lyapunov exponent. At this $xiap(0)$ the stimulus-response curve of $c3^*$ shows a sharp concentration change from an almost linear decrease to zero, which we have defined as a hyperbolic threshold.

For an initial condition of $c8^*(0) = 10^5$ $molecules/cell$, the difference between the global extremum of the MCCs and the other extreme MCCs is much more pronounced, as shown in Fig. 5. A maximum of MCCs is visible only at the smaller critical $xiap(0)$. For this initial value, $c3^*$ has a hyperbolic threshold for all three time points.

Comparing our results for the FTLs and MCCs, in order to identify thresholds in the transient dynamics of the apoptosis decision network, shows that the maxima of the two largest FTLs are found at two critical $xiap(0)$ where also some MCCs have extreme values. The larger value of $xiap(0)$ is located close to the inflection points of $c8^*$, $c3$ and $[c8^*, c3]$. The smaller $xiap(0)$ is located close to the inflection point of $xiap$ and for $c8^*(0) = 5 \cdot 10^4$ $molecules/cell$, $t = 6h$ it is also close to the inflection point of $c3$. Both measures have qualitatively identified the same two critical $xiap(0)$ as thresholds in the transient dynamics. However, there is a quantitative difference: The largest FTL has identified a critical $xiap(0)$, where some MCCs have extreme values too but they do not form the global extremum of the MCCs. In contrast, the maximum of the second largest FTL is found at the same critical $xiap(0)$ as the global extremum of the MCCs. This difference drastically increases with increasing $c8^*(0)$. The value of the critical $xiap(0)$ with the global extremum of the MCCs depends on time such that the chance for survival increases with time which appears biologically unrealistic. The value of the critical $xiap(0)$ with the maximum of the largest FTL is independent of time and is thus more likely to be a biological threshold.

5 Gene transcription network

The question arises whether there are alternative model structures whose transient dynamics are characterized by activation thresholds. Systems with cooperativity can show sigmoidal stimulus-response curves, which suggests them as promising candidates. Cooperativity is a property of many gene transcription networks [30]. We therefore study in this section a simple example for a gene transcription net-

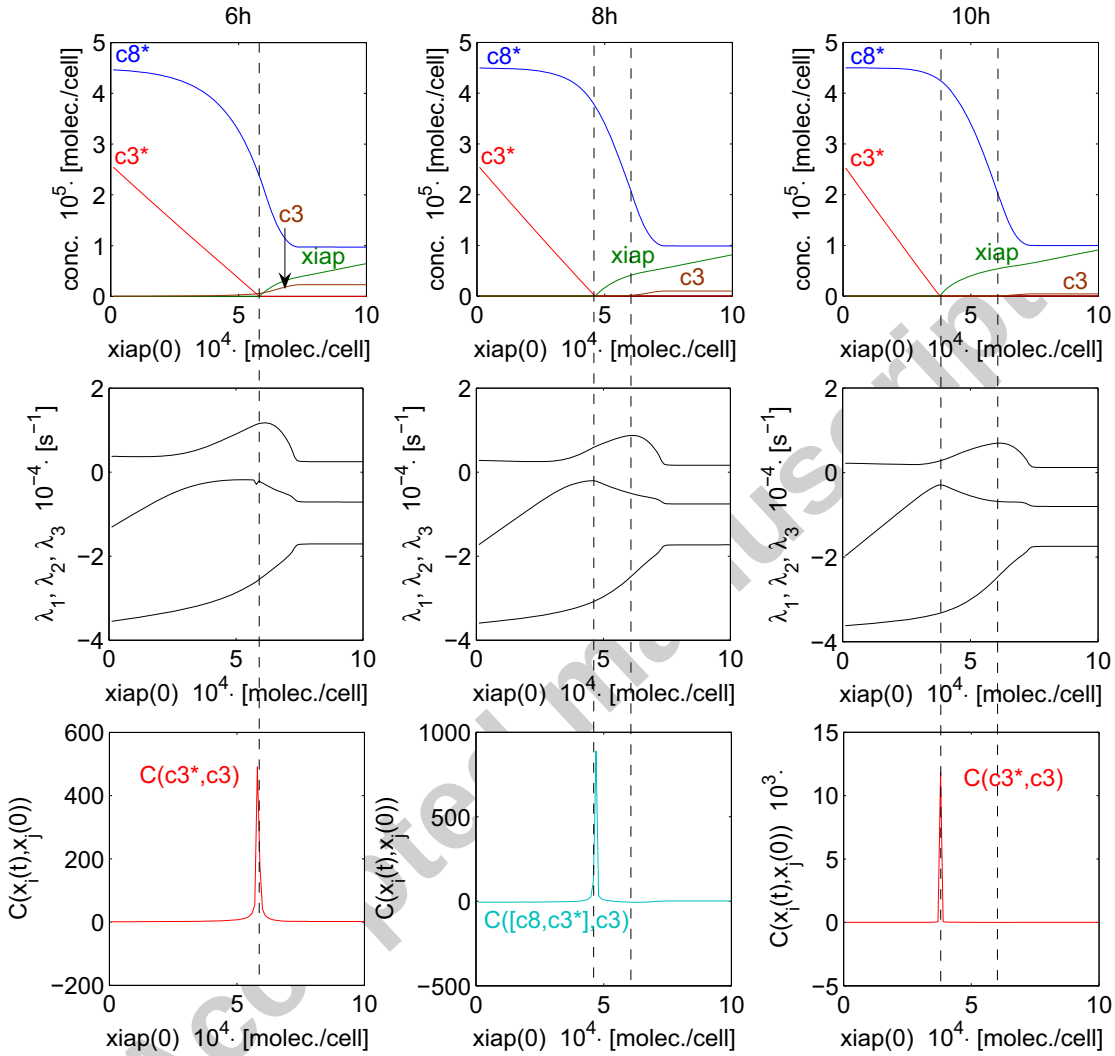

Figure 5: Apoptosis decision network. Quantitative measures to characterize transient dynamics. $c8^*(0) = 10^5$ *molecules/cell*. Abscissa: $xiap(0)$. First row: stimulus-response curve, second row: FTLs and third row: Profiles of MCCs which lead to largest extreme values are shown. Columns: different time points. Dashed lines have been added for a better comparison of the maxima of FTLs, extreme values of MCCs and thresholds in stimulus-response curves. Same colors are chosen for the same response variable in the first and third row. The quantified threshold values are summarized in Table 4 in Appendix A.

work. The temporal concentration changes of the network components are described by the following set of ODE (Model I):

$$\begin{aligned} \dot{x}_1 &= -x_1 \\ \dot{x}_2 &= x_1 \cdot (10 - x_2) - x_2 \qquad \text{Model I} \\ \dot{x}_3 &= 10 \cdot \frac{x_2^4}{1 + x_2^4} - x_3 \,. \end{aligned} \tag{5}$$

The first equation describes the degradation of a stimulus x_1, the second the activation of transcription factor x_2 by x_1 and the third gene transcription activated by x_2, where we have chosen the value four for the Hill-coefficient, which is the cooperativity measure. All variables represent concentrations but without units. In contrast to the example in the previous section, the transient response is induced by a transient stimulus x_1 in this model. In addition we study two extended versions of this network by independently adding different feedback loops. In Model II the deactivation of x_2 is controlled by x_3, while in Model III a positive feedback enhances the activation of x_2 by x_3. The modified equations are

$$\begin{aligned} \dot{x}_2 &= x_1 \cdot (10 - x_2) - x_2 \cdot x_3 \qquad \text{Model II} \\ \dot{x}_2 &= (x_1 + x_3) \cdot (10 - x_2) - x_2 \quad \text{Model III} \,. \end{aligned} \tag{6}$$

The initial condition of the stimulus $x_1(0)$ will be varied to identify a critical value which could form an activation threshold for the output $x_3(t)$. For the other initial conditions we have chosen $x_2(0) = x_3(0) = 0$. The trajectories for x_2 and x_3 of the three models for different $x_1(0)$ are shown in Fig. 6. The trajectories of x_3 for Models I and III show a clustering into two groups during the transients. It is difficult to detect a clustering for Model II but we will later see that the stimulus-response curve of x_3 is sigmoidal[4]. We have chosen time point $t = 2$ to study the transient dynamics.

The related quantitative measures are presented in Fig. 7, where we compare the stimulus-response curves with the spectrum of the FTLs and with the MCCs. The stimulus-response curves are sigmoidal for x_3 in all three models and for x_2 in Model III.

The largest FTL has a maximum at the inflection point of the stimulus-response curves of x_3 in each model. It therefore identifies putative activation thresholds in the transient dynamics for these examples too, though a threshold was hard to detect in the trajectories of Model II. Note, that there is in general no one-to-one

[4]The clustering is more pronounced for a higher Hill-coefficient. In order to study whether quantitative measures can predict thresholds that are difficult to see by visual inspection, we preferred a moderate value, which is still greater than a typical case of a dimer. To see whether this holds for all cases requires confirmation by experiments.

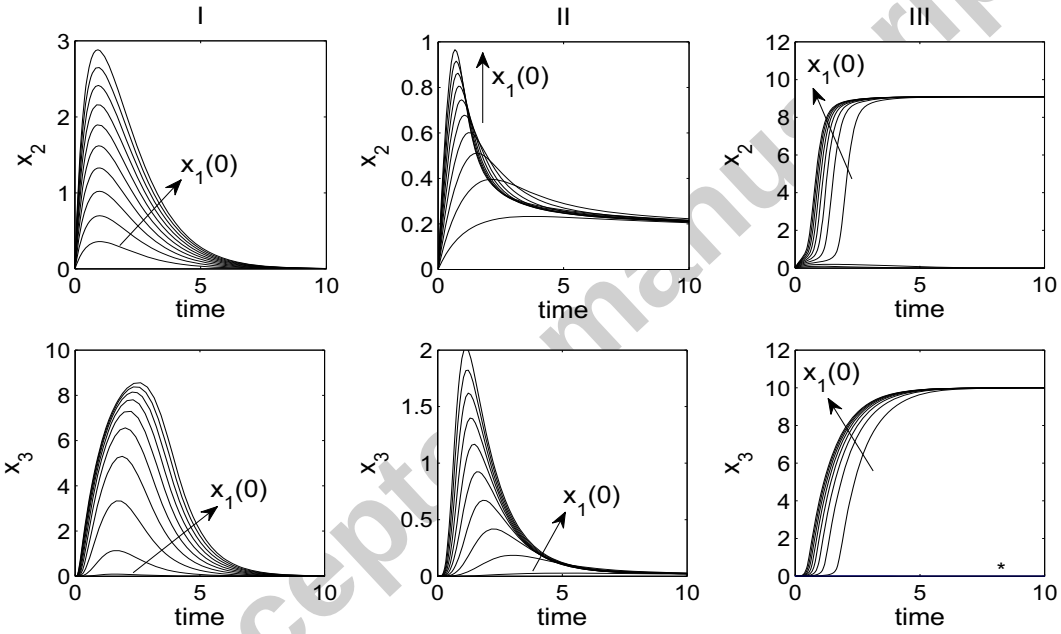

Figure 6: Gene transcription network. Trajectories. First column: without feedback regulation, second column: control of deactivation of x_2, third column: positive feedback. The different curves result from $x_1(0) = 0.1, 0.2, \ldots, 1$ for the first column and from $x_1(0) = 0.025, 0.05, \ldots, 0.25$ for the second and third column and with $x_2(0) = 0$ and $x_3(0) = 0$ for all columns. An arrow indicates the direction of increasing $x_1(0)$. A "*" indicates a cluster of overlapping trajectories. The variables are without unit.

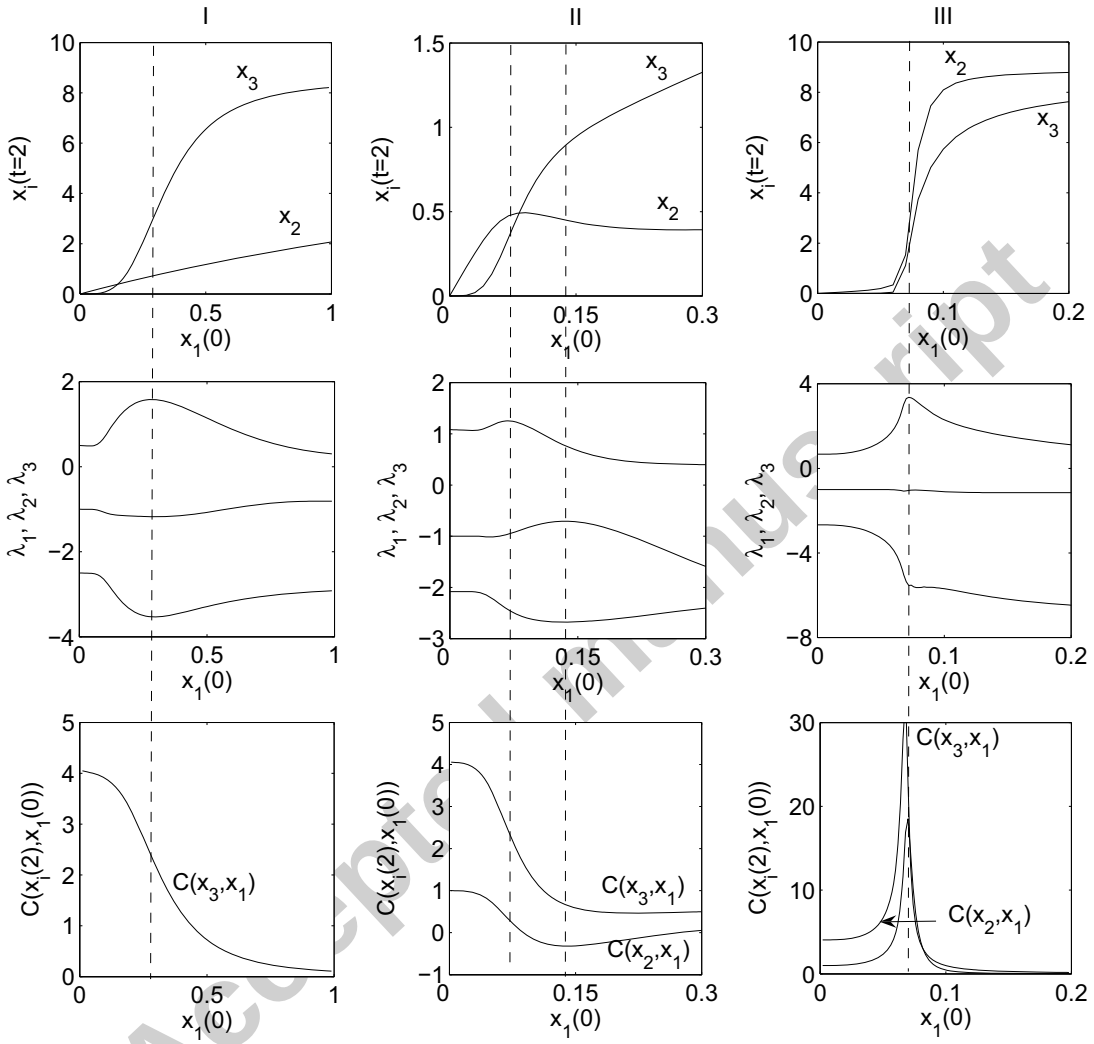

Figure 7: Gene transcription network. Transient response at $t = 2$ in dependence on $x_1(0)$ (abscissa). First column: without feedback regulation, second column: control of deactivation, third column: positive feedback. First row: Stimulus-response curves, second row: Spectrum of FTLs and third row MCCs. Dashed lines have been added for a better comparison of the maxima of the FTLs,the extreme values of MCCs and thresholds in stimulus-response curves.

correspondence between the FTLs and the variables. For the model without feedback, the dynamics of x_3 is also reflected in λ_2 and λ_3. This can easily be verified by removing the equation for x_3 from Eqs. (5). The resulting two-dimensional model leads to two monotonously decreasing FTLs.

The maximum of the largest FTL is preserved over a large time interval during the transient signal as shown for the model without feedback in Fig. 8. Thus the threshold is a temporal robust property of the system.

For the two feedback models the maximal λ_1 is shifted to lower values of $x_1(0)$ as shown in the second and third column of Fig. 7. For Model II, the second Lyapunov exponent λ_2 shows a maximum at a higher critical $x_1(0)$ than the respective value for the maximum of λ_1. The stimulus-response curve of x_2 has the inflection point of a sigmoidal decreasing part at this value which could be related to a stabilization of the trajectory induced by the controlled deactivation of x_2 by x_3, acting for $x_3 > 1$ as a negative feedback, while for $x_3 < 1$ as positive feedback, according to Eq. (6). The other variables could also influence the profile of λ_2. This one can also see for Model III, where only λ_1 shows a maximum and the stimulus-response curves of x_2 and x_3 are sigmoidal with their inflection points at the same $x_1(0)$.

For Models I and II, the curve of the MCC $C(x_3, x_1)$ is monotonously decreasing over the whole $x_1(0)$ interval, as shown in the last row of Fig. 7. For these two models $C(x_3, x_1)$ is not sensitive enough to identify thresholds in the transient dynamics. The positive feedback regulation (Model III) enhances the strength of the activation threshold by showing maxima in $C(x_2, x_1)$ and $C(x_3, x_1)$. For Model II, $C(x_2, x_1)$ has a negative minimal value at the inflection point of the sigmoidal decreasing part of the respective stimulus-response curve.

So far we have studied this gene transcription network for the initial conditions $x_2(0) = 0$ and $x_3(0) = 0$. Due to activation by other enzymes or transcription factors it could be possible that initial values of proteins or mRNA are greater than zero. The results for Model I, with two positive $x_3(0)$, are shown in Fig. 9. The profile of the stimulus-response curve and of the largest FTL are robust against different $x_3(0)$ but the profiles of the MCCs $C(x_3, x_1)$ show a maximum whose position $x_1(0)$ increases with increasing $x_3(0)$[5].

Our investigation of the gene transcription network has thus shown qualitative differences between FTLs and MCCs regarding the identification of thresholds in the transient dynamics. The FTLs have identified the inflection point of the sigmoidal stimulus-response curves as a threshold. The MCC $C(x_3, x_1)$ with $x_3(0) = 0$ is monotonous for Models I and II. The results for the FTLs are robust

[5]In Fig. 9, merging the two figures of each row into one figure, then no visible differences can be seen for x_3 and λ_1. The maximum of the two curves for $C(x_3, x_1)$ are found at different positions, which are close to the interval with the highest curvature of the stimulus-response curve for x_3.

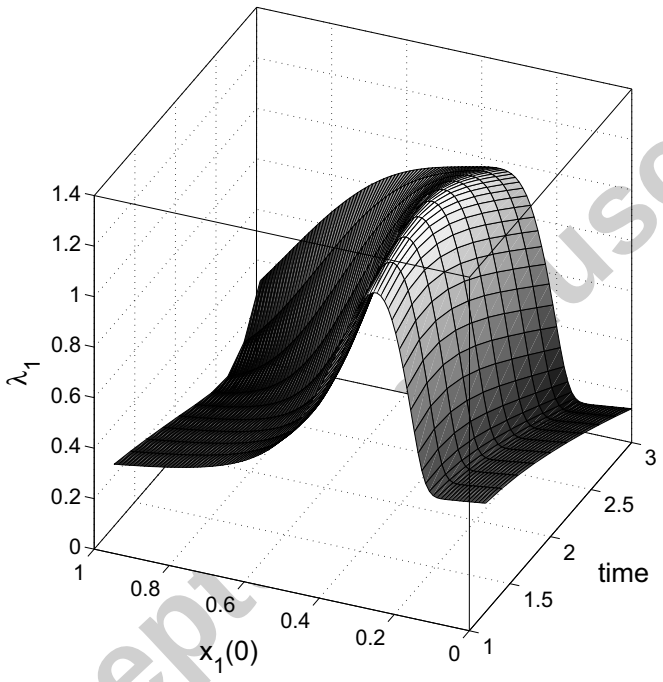

Figure 8: Gene transcription network, Model I, transient response. Largest FTL has a maximum for a broad time interval. Parameters as in the left column of Fig. 7.

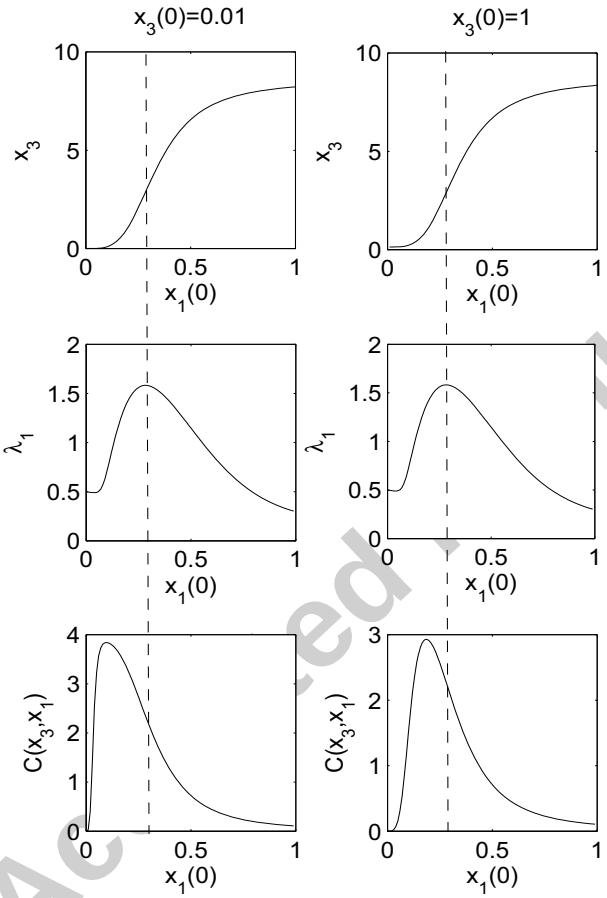

Figure 9: Gene transcription network, Model I. Transient response at $t = 2$ for different $x_3(0)$ in dependence on $x_1(0)$ (abscissa). First column: $x_3(0) = 0.01$, second column: $x_3(0) = 1$.

for different initial $x_3(0)$ while the profile of the MCC shows a maximum whose position $x_1(0)$ depends on the initial value $x_3(0)$. Thus the MCCs do not reliably detect all thresholds and suffer from false positives.

6 The threshold of the Hill equation

Our analysis of the gene transcription network without feedback has shown that the MCC $C(x_3, x_1)$ is monotonously decreasing with increasing stimulus $x_1(0)$ for the default case with $x_3(0) = 0$ but shows a maximum for a positive $x_3(0)$ whose position $x_1(0)$ is proportional to $x_3(0)$. This property motivated our analytical investigation of the MCC, the FTL and two other quantitative measures from the literature for a Hill curve with a positive response for a zero input. A positive response for zero input could have been induced by other transcription factors in case of gene transcription. The Hill equation is a standard example of a sigmoidal stimulus-response curve. With a positive initial response b, it is defined by the following equation

$$y = f(x) = b + x^n/(1 + x^n)\,. \tag{7}$$

Assuming that the stimulus-response curve of a one-dimensional mathematical model can be described by the Hill equation with a Hill coefficient $n \geq 2$ at a time point during the transient dynamics or in the steady state. Then the FTL has its maximum at the stimulus with the inflection point of the Hill equation. Thus the position of the maximum of the FTL is independent of a positive initial response b. A right translation of the Hill curve would also change the position of the maximum of the FTL but not its value. The cooperativity index $f^{-1}(0.9)/f^{-1}(0.1)$ is also independent of a positive initial response but its value depends on a right translation of the Hill curve [8].

Perturbing the stimulus x by h percent and inserting Eq. (7) in Eq. (1) results in the following equation for the MCC

$$C(f(x), x) = C(x) \quad = \left(\frac{(b + x^n(1 + b)(1 + h)^n)(1 + x^n)}{(1 + x^n(1 + h)^n)(b + x^n(1 + b))} - 1 \right) \frac{1}{h}\,. \tag{8}$$

Next we calculate the stimulus x with the maximum of $C(x)$:

$$\frac{d}{dx}C(x) = \frac{n((1 + h)^n - 1)(b - (1 + b)(1 + h)^n x^{2n})x^{n-1}}{(b + x^n(b(1 + h)^n + 1 + b) + (1 + b)(1 + h)^n x^{2n})^2 h}$$

with the roots at

$$x_1 = 0 \quad \text{and} \quad x_2 = \left(\frac{b}{(1 + b)(1 + h)^n} \right)^{1/2n}\,. \tag{9}$$

Finally

$$\frac{d^2}{dx^2}C = \frac{(b^2(n-1) - bpx^n - 4bnqx^{2n} + pq(1-2n)x^{3n} + q^2(1-n)x^{4n})x^{n-2}}{(b + px^n + qx^{2n})^3 h}$$
$$\frac{d^2}{dx^2}C(x_2) < 0 \quad \text{and} \quad \frac{d^2}{dx^2}C(x_1) = 0$$
$$\text{with} \quad p = b(1+h)^n + b + 1 \quad \text{and} \quad q = (1+b)(1+h)^n\,. \tag{10}$$

Our result of Eq. (9) shows that the MCC $C(f(x), x)$ for the Hill curve without a positive initial response does not have any extreme value for $x > 0$. If the Hill curve has a positive initial response then the MCC has a maximum whose position x depends on the value of the initial response, as shown by Eqs. (9) and (10). Thus a maximum of the MCC neither detects the inflection point, nor the interval of the highest curvature hyperbolic threshold whose positions are independent of b.

Alternatively, the Hill equation can be defined with a basal activity which could correspond to a basal transcription rate or a basal rate for phosphorylation. The transcription rate or the phosphorylation rate have a maximum independent on the basal activity which is different to the first model where the maximal activation is proportional to the initial positive response. Introducing a basal activity leads to the following form of the Hill equation:

$$y = f(x) = b + (1-b)x^n/(1+x^n)\,. \tag{11}$$

For the MCC it follows that

$$C(f(x), x) = C(x) = \left(\frac{(b + (1+h)^n x^n)(1+x^n)}{(1 + (1+h)^n x^n)(b + x^n)} - 1\right)\frac{1}{h}$$
$$\frac{d}{dx}C(x) = \frac{(b - (1+h)^n x^{2n})(b + (1+h)^n(1-b) - 1)nx^{n-1}}{(b + ((1+h)^n b + 1)x^n + (1+h)^n x^{2n})^2 h}$$

with the root leading to a maximum at

$$x = \left(\frac{b}{(1+h)^n}\right)^{1/2n}\,. \tag{12}$$

The MCC has a maximum for a positive basal activity for this definition of a Hill equation too.

The Hill equation on its own is frequently used to quantify ultrasensitivity in biochemical networks by fitting the Hill equation to the stimulus-response curve of a network. However this approach is not appropriate if the response exhibits basal activation [29]. An alternative approach to quantify sensitivities of networks with

basal activity has been introduced in [29]. The authors have defined the MCC as a function of the activated fraction f (Eq. (7) in [29])

$$C(f) = n\frac{(1-f)f(1-b)}{b+f(1-b)} \quad \text{with} \quad f = \frac{x^n}{1+x^n}\,. \tag{13}$$

The response as a function of the activated fraction shows a maximum at

$$f = \frac{1}{1-b}\left(-b + \sqrt{b^2+b(1-b)}\right)\,. \tag{14}$$

The result is similar to the results for the MCC according to Eqs. (9) and (12): The response coefficient of Eq. (13) has a maximum at a critical f whose position depends on the basal activity and the maximum vanishes for zero basal activity.

In experiments, cells are frequently starved to study their response to a specific stimulation profile, without the influence of basal activity or without the influence of a positive initial response. The reason for this is that a signaling pathway can be active without stimulation in a cell culture. Our analysis has shown that quantifying the response by the MCC, or by the response coefficient of Eq. (13), can lead to qualitatively different results for experiments with and without starvation. In contrast, a maximum of the FTL identifies the increasing part of a stimulus-response curve and is thus robust against changes of basal activities or against a positive initial response, as our results for the gene transcription network of Eqs. (5) have shown (Fig. 9).

7 Most unstable direction of relative changes

The investigated examples have shown differences of the two quantitative measures regarding the prediction of thresholds in transient dynamics, which could be related to the different properties of these two measures (Section 2): The FTLs identify the most unstable direction of the state space and the stability in all orthogonal directions on the basis of absolute distances between the trajectory and perturbed trajectories. The MCCs measure the response-perturbation ratio on the basis of relative changes of state variables.

In this section, we introduce an alternative measure which combines properties of the FTL and of the MCC: The most unstable direction of the state space is a useful property of biochemical networks with overlapping stimulus-response curves of different proteins as shown in Fig. 1. We start with the definition of the MCCs according to Eq. (1). The column vectors of Eq. (1) form an orthonormal system for $t = 0$. We calculate the spectral norm SN of Eq. (1) according to

$$SN(t, x_0) = \sqrt{\Lambda_{max}(C^T \cdot C)}\,, \tag{15}$$

where $\Lambda_{max}(C^T \cdot C)$ denotes the largest eigenvalue of $C^T \cdot C$. The eigenvector associated with the largest eigenvalue has the maximal stretching. Thus the SN identifies the most unstable direction of the relative changes $\partial \log x_i(t)/\partial \log x_j(0)$. The value of the SN depends on the size of the percentaged perturbation of the $x_j(0)$. For perturbations of one percent or less the differences are negligible in our studied examples.

In analogy to the largest FTL we define the relative instability exponent RIE by

$$RIE(t, x_0) = \frac{1}{t} \log(SN) \,. \tag{16}$$

The motivation for this is as follows. While the spectral norm helps us to identify the maximal stretching, taking the logarithm and dividing by time ensures that the profiles obtained are comparable to the largest FTL.

The following example illustrates the differences between FTL and RIE: $\dot{x} = cx$. We obtain a FTL equal to c and $RIE = \log(1)/t = 0$. This is due to the fact that the system variable and the perturbation evolve according to the same equation, which leads to a value for RIE equal to zero.

Fig. 10 shows the RIE of the apoptosis decision network for the same parameters which have been used in Figs. 4 and 5. The RIE shows maxima at the same critical $xiap(0)$, where the FTLs and MCCs show extreme values too. For the two later time points the RIE at the sigmoidal threshold of $xiap$ is greater than the RIE at the sigmoidal threshold of $c8^*$ in three of four cases. Thus for this example the profile of the RIE is more similar to the profile of the MCCs than to the profile of the FTLs.

The RIE for the gene transcription network without feedback is shown in Fig. 11 for three different $x_3(0)$. The RIE sensitively depends on this initial condition. Its curve has a similar profile as the curves of the MCC $C(x_3, x_1)$ in Figs. 8 and 9.

Our two examples have shown that the dependence of the RIE on the stimulus is more influenced by the relative changes than by the most unstable direction. From our discussion and comparison of quantitative measures it follows that the RIE is less appropriate to identify thresholds in transient signaling, suggesting that quantitative measures introduced to identify thresholds in transient signaling should be defined on the basis of absolute differences between trajectories and perturbed trajectories.

8 Summary and conclusions

We investigated transient dynamics of mathematical models describing biochemical networks and compared quantitative measures to identify thresholds in transient responses. Thresholds separate different behaviors of a system. Sigmoidal

stimulus-response curves are considered as typical thresholds in biochemical networks. We examined a mathematical model of an apoptosis decision network (mutual activation cycle) and of a gene transcription network (cooperative regulation) as well as the Hill equation that can show thresholds in their transient dynamics. We then compared finite-time Lyapunov exponents (FTL) with transient metabolic control coefficients (MCC) as quantitative measures to predict thresholds in the dynamics of these networks.

We obtained the following results: A maximum of an FTL identifies the value of an external stimulus or an initial condition, leading to the inflection point of a sigmoidal stimulus-response curve. In case of overlapping sigmoidal stimulus-response curves a FTL identifies a stimulus value close to the different inflection points of the responses. The largest FTL can identify a different threshold value than the second largest FTL, which are related to stimulus-response curves with nonoverlapping rising parts.

For the gene transcription network and for the Hill equation our results demonstrate that at the stimulus value, where the respective stimulus-response curve has an inflection point, in several cases the MCCs have no extreme values. Furthermore, some MCCs have extreme values at stimuli where the respective stimulus-response curve has no point of inflection and in two cases they show extreme values near the interval with the highest curvature.

The FTLs are robust against variations of initial values of network components which are not the stimulus of the relevant stimulus-response curves. The profiles of the MCCs can depend on the initial values of other components, as shown for the gene transcription network and the Hill equation. These results are important for experimental studies of signalling pathways under starvation because mathematical models, based on data from experiments either with or without starvation, could show different sensitivities.

The different results for FTLs and MCCs are related to the different properties of these two measures. We introduced the relative instability exponent, called RIE. The RIE identifies the most unstable direction of relative changes. Our analysis led to the result that the RIE shares more properties with the MCCs than with the FTLs and is therefore not appropriate to identify thresholds.

We investigated examples which are complex enough to show thresholds in transient signaling but at the same time allow us to compare in detail the dynamics of the trajectories with respect to the FTLs and MCCs. In large biochemical networks such a detailed comparison would be very time consuming. Therefore quantitative measures to identify putative thresholds in the transient dynamics are required. Our investigation suggests that they should identify the most unstable direction and that they should be defined on the basis of absolute differences between responses. The spectrum of the finite-time Lyapunov exponents unambigu-

ously and reliably identifies putative thresholds as inflection points of sigmoidal stimulus-response curves in transient dynamics. Relative measures, like metabolic control coefficients, do not reliably detect all thresholds and suffer from false positives. A consequence for biochemical networks that show relative responses, is that FTLs are needed to identify thresholds, while MCCs should be applied to compare the amplitude of different thresholds.

Finally we discuss the application of FTLs and MCCs for the prediction of therapeutical interventions in biochemical networks [31]. For mitochondrial diseases it has been shown that the hyperbolic threshold for the inhibition of different mitochondrial complexes is a linear decreasing function of the respective flux control coefficient [32]. However, it has not been studied whether a threshold can be identified by extreme values of the MCCs.

For the administration of a drug, which binds as an extracellular ligand to a specific receptor on the cell membrane, the dose of the drug must exceed a threshold to activate the intracellular biochemical network. On the other hand, the dose of the drug should not be higher than necessary to avoid unwanted side effects. A maximum of an FTL can identify the minimal initial concentration of a drug that leads to the activation of a downstream network. FTL could also support the design of dose split experiments to avoid that the dose is decreasing below a threshold value. The threshold value could have changed over time due to changes of intracellular protein concentrations.

MCCs are applicable in medical systems biology for a comparison of the responses of different state variables in dependence on perturbations of different parameters or initial conditions of state variables [33]. Such perturbations could be induced by small molecules. In case that one is interested in a measure summarizing the responses of all variables the RIE could be useful. Global methods of sensitivity analysis need to be applied to study simultaneous perturbations of several initial conditions,[20]. A comparison with the result for the RIE would be interesting.

FTLs and MCCs can also be applied in combination to support the design of experiments in systems biology: An analysis of MCC leads to the identification of drugs or small molecules which most effectively perturb a biochemical network. Then FTLs will determine the optimal stimulus profile of a drug or small molecule.

A Quantified threshold values

In the following two tables we summarize the values for $xiap(0)$ leading to maxima of the largest and second largest FTL and to extreme values of the MCCs in Figs. 4 and 5.

Row in Fig. 4	component	6h	12h	18h
inflection point	$c8^*$	45	44	44
	$c3$	46	46	46
FTL	λ_1	45	44	44
MCC	$C(c8^*, c3)$, $C(c3, c3)$	46	45	45
inflection point	$c3^*$	45		
	$xiap$	46	34	23
highest curvature	$c3^*$		33	33
FTL	λ_2	45	32	25
MCC	$C(xiap, c3)$, $C(c3^*, c3)$	46	33	22

Table 3: Apoptosis decision network: $xiap(0)$ in 10^4 *molecules/cell* leading to maximal FTLs and extreme values of MCCs in Fig. 4.

Row in Fig. 5	component	6h	8h	10h
inflection point	$c8^*$	60	60	60
	$c3$	66	67	68
FTL	λ_1	61	62	61
MCC				
inflection point	$c3^*$	57		
	$xiap$	60	48	39
highest curvature	$c3^*$		45	37
FTL	λ_2	55	45	38
MCC	$C(c3^*, c3)$	58		38
	$C([c8, c3^*], c3)$		47	

Table 4: Apoptosis decision network: $xiap(0)$ in 10^4 *molecules/cell* leading to maximal FTLs and extreme values of MCC in Fig. 5.

B Maximum of negative FTL

The dynamics of the following one-dimensional example $\dot{x} = -x/(1+x^6) - x$ leads to a maximum of a negative FTL . The trajectories and the FTL are shown in Fig. 12

Acknowledgements

K.R. acknowledges support by the German Ministry for Education and Research (BMBF) through the FORSYS junior research group programme (grant number 0315255). O.W. received support through the Helmholtz Alliance on Systems Biology and acknowledges support by the Stellenbosch Institute for Advanced Study (STIAS), South Africa. We thank M. Harle, T. Millat, M. Swat, N. Blüthgen, J. Snoep, F. Winter and R. Klages for useful discussions.

References

[1] Heinrich, R., and Schuster, S.: 'The Regulation of Cellular Systems', (Chapmann and Hall, 1996)

[2] Aldridge, B.B., Haller, G., Sorger, P.K., and Lauffenburger, D.A.: 'Direct Lyapunov exponent analysis enables parametric study of transient signaling governing cell behavior', *IEE Proc Syst Biol*, 2006, **153**, pp., 425–432

[3] Bolouri, H., and Davidson, E.H.: 'Transcriptional regulatory cascades in development: initial rates, not steady state, determine network kinetics', *Proc Natl Acad Sci*, 2003, **100**, pp. 9371–9376

[4] Kao, S., Jaiswal, R.K., Kolch W., and Landreth, G.E.: 'Identification of the mechanisms regulating the differential activation of the mapk cascade by epidermal growth factor and nerve growth factor in PC12 cells', *J Biol Chem*, 2001, **276**, pp. 18169–18177

[5] Cheong, R., Bergmann. A., Werner, S.L., Regal, J., Hoffmann, A., and Levchenko, A.: 'Transient IKK activity mediates NF-κB temporal dynamics in response to a wide range of TNFα doses', *J Bio Chem*, 2005, **281**, pp. 2945–50

[6] Hao, N., Yildirim, N., Wang, Y., Elston, T.C., and Dohlman, H.G.: 'Regulators of G protein signaling and transient activation of signaling: experimental and computational analysis reveals negative and positive feedback controls on G protein activity', *J Biol Chem*, 2003, **278**, pp. 46506–46515

[7] Sasagawa, S., Ozaki, Y.I., Fujita, K., and Kuroda, S.: 'Prediction and validation of the distinct dynamics of transient and sustained ERK activation', *Nat Cell Biol*, 2005, **7**, pp. 365–373

[8] Goldbeter, A., and Koshland, D.E.: 'An amplified sensitivity arising from covalent modification in biological systems', *Proc Natl Acad Sci USA*, 1981, **78**, pp. 6840–6844

[9] Ferrell J.E.: 'Tripping the switch fantastic: how a protein kinase cascade can convert graded input into switch-like outputs', *TIBS*, 1996, **21**, pp. 640–466

[10] Buchler N.E., and Cross, F.R.: 'Protein sequestation generates a flexible ultrasensitive response in a genetic network', *Mol Sys Biol*, 2009, 5:272

[11] Ferrell, J.E., and Machleder, E.M.: 'The biochemical basis of an all-or-none cell fate switch in Xenopus oocytes', *Science*, 1998, **280**, pp. 895–898

[12] Nash, P., Tang, X., Orlicky, S., Chen, Q., Gertler, F.B., Mendenhall, M.D., Sicheri, F., Pawson, T., and Tyers, M.: 'Multisite phosphorylation of a CDK inhibitor sets a threshold for the onset of DNA replication', *Nature*, 2001, **414**, pp. 514–521

[13] Bhalla, U.S., Ram, T.P., and Iyengar, R.: 'MAP kinase phosphatase as a locus of flexibility in a mitogen activated protein kinase signaling network', *Science*, 2002, **297**, pp. 1018–1023

[14] Huang, C.Y.F., and Ferrell, J.E.: 'Ultrasensitivity in the mitogen-activated protein kinase cascade', *Proc Natl Acad Sci USA*, 1996, **93**, pp. 10078–10083

[15] Bentele, M., Lavrik, I., Ulrich, M., Stosser, S., Heermann, D.W., Kalthoff, H., Krammer, P.H., and Eils, R.: 'Mathematical modeling reveals threshold mechanism in CD95-induced apoptosis', *J Cell Biol*, 2004, **166**, pp. 839–851

[16] Gunarwardena, J.: 'Multisite protein phosphorylation makes a good threshold but can be a poor switch', *Proc Natl Acad Sci USA*, 2005, **102**, pp. 14617–14622

[17] Salazar, C., and Höfer, T.: 'Versatile regulation of multisite protein phosphorylation by the order of phosphate processing and protein-protein interactions', *FEBS Journal*, 2007, **274**, pp. 1046–1061

[18] Ingalls, B.P., and Sauro, H.M.: 'Sensitivity analysis of stoichiometric networks: an extension of metabolic control analysis to non-steady state trajectories', *J Theor Biol*, 2003, **222**, pp., 23–36

[19] Hornberg, J.J., Bruggeman, F.J., Binder, B., Geest, C.R., Vaate, A.J.M.B. de., Lankelma, J., Heinrich, R., and Westerhoff, H.V.: 'Principles behind the multifarious control of signal transduction ERK phosphorylation and kinase/phosphatase control', *FEBS Journal*, 2005, **272**, pp., 244–258

[20] Zhang, Y., and Rundell, A.: 'Comparative study of parameter sensitivity analyses of the TCR-activated Erk-MAPK signaling pathway', *IEE Proc Syst Biol* Sy 2006, **153**, pp. 210–211

[21] Eckmann, J.P., and Ruelle, D.: 'Ergodic theory of chaos and strange attractors', *Reviews of Modern Physics*, 1985, **57**, pp. 617–656

[22] Grassberger, P., Badii, R., and Politi, A.: 'Scaling laws for invariant measures on hyperbolic and nonhyperbolic attractors', *Journal of Statistical Physics*, 1988, **51**, pp. 135–178

[23] Ott, E.: 'Chaos in dynamical systems', (Cambridge University Press, 1994)

[24] Abarbanel, H.D.I.: 'Analysis of observed chaotic data', (Springer, New York, 1996)

[25] Haller, G.: 'Distinguished material surfaces and coherent structures in three-dimensional fluid flows', *Physica D*, 2001, **149**, pp. 248–277

[26] Cohen-Saidon, A, Cohen A.A., Sigal, A., Liron, Y., and Alon, U.: 'Dynamics and Variability of ERK2 Response to EGF in individual Living Cells', *Molecular Cell*, 2009, **36**, pp. 885–893

[27] Shinar G., Milo, R., Martinez, M.R., and Alon, U.: 'Input output robustness in simple bacterial signaling systems', *Proc Natl Acad Sci USA*, 2007, **104**, pp. 19931–19935

[28] The MathWorks Inc. Matlab 7.5.0 R2007b 2007. www.mathworks.com

[29] Legewie, S., Blüthgen, N., and Herzel, H.: 'Quantitative analysis of ultrasensitive response', *FEBS Journal*, 2005, **272**, pp. 4071–4079

[30] Courey, A.: 'Cooperativity in transcriptional control', *Current Biology*, 2001, **11**, pp. 250–252

[31] Wolkenhauer, O., Fell, D., De Meyts, P., Bluethgen, N., Herzel, H., Le Novere, N., Hoefer, T., Schuerrle, K., and van Leeuwen, I.: 'SysBioMed report: Advancing systems biology for medical application', *IET Syst. Biol.*, 2009, **3**, pp. 131-136

[32] Mazat, J.P., Rossignol, R., Malgat, M., Rocher, C., Faustin, B., and Letellier, T.: 'What do mitochondrial diseases teach us about normal mitochondrial functions... that we already knew: threshold expression of mitochondrial defects', *Biochimica et Biophysica Acta*, 2001, **1504**, pp. 20–30

[33] Cascante, M., Boros, L.G., Comin-Anduix, B., de Atauri, P., Centelles, J.J., and Lee, P.W.N.: 'Metabolic contol analysis in drug discovery and disease', *Nature Biotechnol.*, 2002, **20**, pp. 243–249

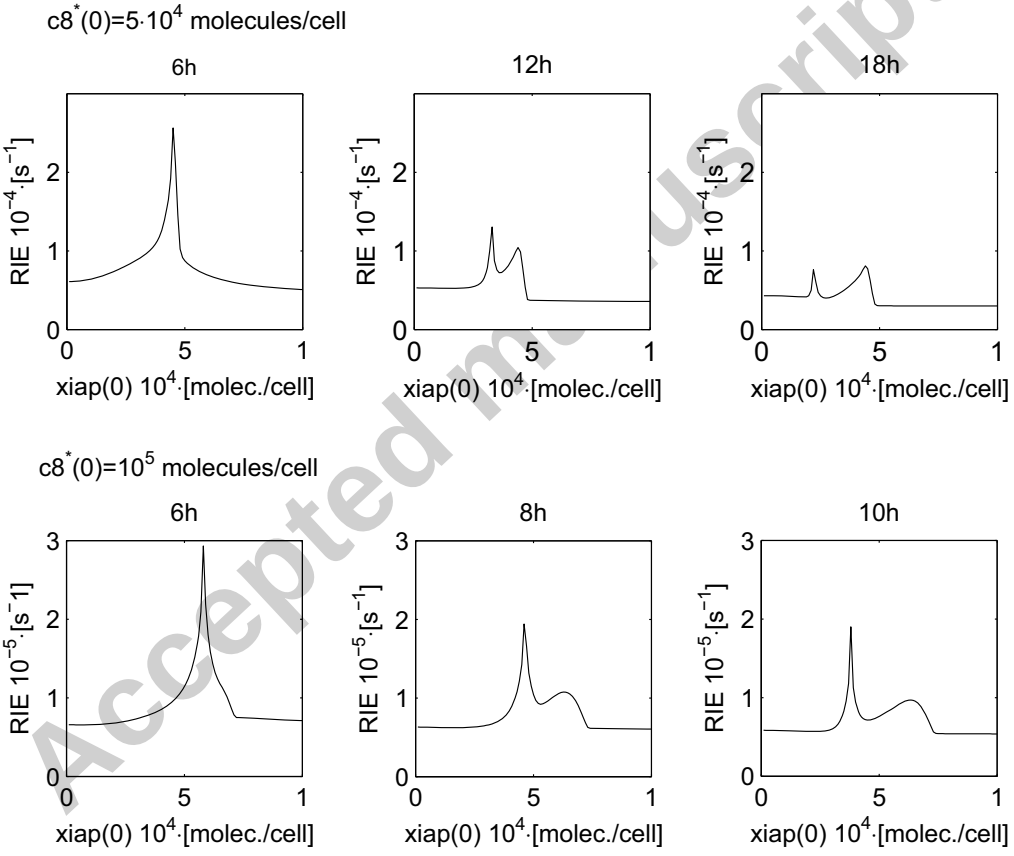

Figure 10: Relative instability exponent (RIE) for the apoptosis decision network.

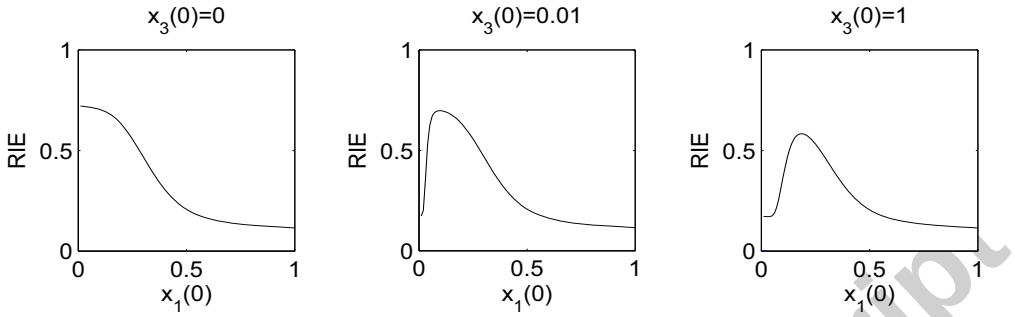

Figure 11: Relative instability exponent (RIE) for the gene transcription network without feedback at $t = 2$.

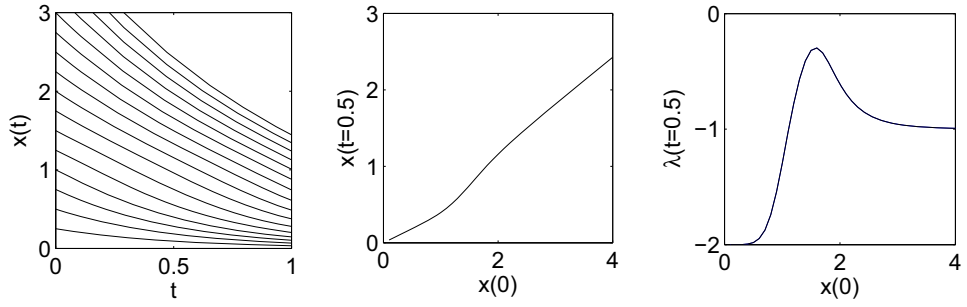

Figure 12: Maximum of a negative FTL.